NATIONAL TRANSPORTATION SAFETY BOARD
Office of Research and Engineering
Materials Laboratory Division
Washington, D.C. 20594

July 16, 2020[1]

MATERIALS LABORATORY FACTUAL REPORT Report No. 19-028

A. ACCIDENT INFORMATION

Place : Dallas, Texas
Date : February 23, 2018
Vehicle : Pipeline operated by Atmos Energy
NTSB No. : PLD18FR002
Investigator : Sara Lyons[2]

B. COMPONENTS EXAMINED

Steel gas main that was installed behind dwelling 3539 Durango Drive. The accident dwelling involved in the gas-fueled explosion was located at 3534 Espanola Drive. The work reflected in this report is a continuation of work that was published in Materials Laboratory Factual Report 18-067.

C. DETAILS OF THE EXAMINATION

Steel Main Behind Dwelling 3539 Durango Drive

According to records from Atmos Energy, the steel main was installed in 1946, and the exterior was specified as spiral wrapped with coal tar enamel coating. Records were not available that would have identified the manufactured date of the main or name of the company that manufactured the main. For the purpose of this examination, the top dead center of the main was at the 12:00 o'clock position.

Bench Binocular Microscope Examination

Figure 1 shows a photograph of the west face of the fracture prior to cleaning. The fracture face at two isolated areas contained a barely visible black regions adjacent to the dent on the external surface, in the areas indicated by regions "S1" and "S2" in figure 1. The west face of the fracture was cleaned with cellulose acetate replica tape. Figure 2 shows the face of the fracture after the replica tape cleaning procedure was repeated four times. The cleaning improved clarity of the black regions and their boundaries. The black regions extended between the outer surface and as deep as approximately 0.07 inch below the surface, to the approximate areas indicated by black dashed lines in figures 1 through 5. The black regions appeared similar to thumbnail-like patterns.

[1] This laboratory report was originally completed on July 24, 2019 but later was revised based on minor comments received during the Technical Review, which was held on July 14, 2020.
[2] The on-site investigators were Ravi Chhatre and Roger Evans. The current investigator-in-charge is Sara Lyons.

SEM Examination

Scanning electron microscope (SEM) examination of the west face of the fracture, prior to any cleaning, revealed the fracture face was covered with soil deposits that obscured the fine fracture features.

SEM examination of the west face of the fracture, after the four-step acetate tape cleaning process described earlier, revealed the outer surface at isolated areas contained evidence of minor shear lips, including areas in the black regions. The inner surface contained minor shear lips outside of the major shear lip regions reported in Materials Laboratory Factual Report 18-067. The general direction of fracture propagation is indicated by arrows in figure 1. The exposed fracture face contained evidence of cleavage fracture features that were pitted. The fracture face contained no evidence of crack arrest fracture features within the black thumbnail region or areas that corresponded to the outline of the black thumbnail-like regions. The crack terminated in the areas indicated by solid lines in figure 1. The fracture features outside of the solid lines in figure 1 were laboratory induced fractures.

After the four-step acetate tape cleaning process, the fracture face was ultrasonic cleaned with Alconox, a commercial detergent, and the fracture face was re-examined with an SEM. SEM examination of the fracture showed fracture features that were similar to those observed after the four-step acetate tape cleaning process.

EDS Analysis

X-ray energy dispersive spectroscopy (EDS) analysis was performed on a soil sample that was collected onsite in the general area of the main, soil sample identified as item “14A”, and on a hard deposit that was removed by the NTSB Materials Laboratory from the surface of gouge “B1”.[3] The hard deposit was removed from the pipe by impacting on the hard deposit with a hammer. After removal from the main, the hard deposit was in the form of a powder.

Appendix 1A shows the overlapping EDS spectra of the two materials (soil sample “14A”” and hard deposit “B1”). EDS analysis of soil sample “14A” produced a spectrum that contained major elemental peaks of oxygen (O), silicon (Si), aluminum (Al), calcium (Ca), and carbon (C) and minor elemental peaks of iron (Fe), magnesium (Mg), potassium (K), and titanium (Ti). The EDS spectrum of hard deposit “B1” contained the same elemental peaks as soil sample “14A” with the exception that the hard deposit “B1” contained an elemental peak of sulfur (S) but no evidence of a magnesium peak. The height of the respective elemental peaks varied between the two samples. The EDS spectrum of the hard deposit “B1” contained a calcium peak that was three times greater, and a carbon peak that was twice as great, compared to those same respective elemental peaks that were found in soil sample “14A”.

[3] Refer to NTSB Materials Laboratory Factual Report No. 18-067, and figures 7, and figures 12 through 14, for the location of gouge “B1”.

Appendix 1B shows an EDS spectrum of the fracture face prior to cleaning prior to cleaning (it is area located outside of the black region). This EDS spectrum was overlapped with an EDS spectrum of the black region, “S1” in figure 2, after replica tape cleaning procedure was repeated four times. The EDS spectrum from the fracture face located outside of the black region (prior to cleaning) contained major elemental peaks of calcium, oxygen, silicon, iron, and carbon, and minor elemental peaks of magnesium, sulfur, potassium, titanium, aluminum, manganese, and zinc. The EDS spectrum from the black deposit contained major elemental peaks of iron, oxygen, and carbon. The elemental peak zinc was found only on the fracture face, prior to and after cleaning with replica tape.

Appendix 1C shows an EDS spectrum of the hard deposit “B1” overlapped with an EDS spectrum from the fracture face prior to cleaning. As a general observation, the EDS spectrum from the fracture face prior to cleaning contained the same elemental peaks as those found on the hard deposit “B1”. The elemental peak intensity of iron on the fracture face (prior to cleaning) was more than three times greater than the intensity of the same peak on the EDS spectrum of the hard deposit. Elemental peak of sulfur was found on the hard deposit and fracture face.

Cross section

A longitudinal-radial section was made through the west face of the fracture in the area that intersected the dent, indicated by section lines “A-A” in figure 2. Another longitudinal-radial section was made through the fracture face in the area that intersected a black region and the dent, indicated by section line “B-B” in figure 2. The prepared sections were ground, polished and etched with 4% Nital reagent. Examination of the sections revealed the outer surface contained evidence of severe metal flow deformation. Figures 6 and 7 show severe metal deformation on the outer surface of the dent in section “A-A”. Appendix 2A at the upper left corner of the page shows an SEM image of a portion of section “B-B in the area that intersected the outer surface of the main. Appendix 2B at the upper left corner of the page shows an SEM image of a portion of section “B-B” in the area that intersected the fracture face and outer diameter surface. The outer surface of section “B-B” exhibited metal flow deformation.

A 0.4-inch long ring portion was cut from the main at a location that was approximately 2 inches west of the dent (see Appendix 4). The west face of this ring portion was ground, polished and macro-etched with 4% Nital reagent. Visual examination of the prepared cross section revealed no evidence of a longitudinal weld seam. The wall at the inner surface and 12 o’clock position contained a narrow band (mark) that ran along the length of the main. A piece of the wall with the longitudinal narrow mark was excised from the ring portion and encased in a metallurgical mount. The metallurgical mount was prepared and etched with 2% Nital reagent. Detailed examination of the prepared section with a metallograph revealed the main contained a microstructure of ferrite and pearlite consistent with steel with no evidence of a longitudinal weld seam. The outer surface of the pipe contained a layer of iron oxide.

Another 0.4-inch long ring portion was cut from the main at a location that was approximately 28 inches east of the west end of the main, (see Appendix 4). The west face was ground, polished and macro-etched with 4% Nital reagent. The etched cross section

contained no evidence of longitudinal weld seam. A 2-inch long ring portion was cut from an area that was adjacent and east of the 0.4-inch long ring portion, (see Appendix 4). The outer surface of the 2-inch long ring portion contained minor evidence of a hard, compacted, adherent deposit that extended around the outer surface. The path of the hard deposit was irregular and did not follow the circumference of the main. The outer surface of 2-inch long ring portion was struck with a brass hammer at two isolated areas, causing the hard deposits to break off at these two areas and exposing the base metal. Visual examination of the 2-inch long ring portion revealed the outer surface at the two exposed areas and the inner surface contained no evidence of weld beads.

X-ray Dot Map

Appendix 2A shows an X-ray dot map of the hard deposit that was found on the surface of the dent, in the area indicated by cross section “B-B” in figure 2. The section was encased in plastic and coated by vapor deposition with gold-palladium. The major portion of the hard deposit contained calcium (element with the greatest distribution throughout the matrix). The hard deposit contained irregular-isolated areas of silicon with the same respective locations containing oxygen, consistent with particles of silicon oxide. The hard deposit also contained carbon, and minor amounts of aluminum and magnesium, but these three elements appeared did not share the same respective positions. The X-ray dot map showed that the wall of the main was primarily iron consistent with a main that was made from a ferrous alloy such as steel.

Appendix 2B shows X-ray dot map of a portion of the fracture face where it intersected the outer surface of the main, prepared from cross section “B-B” in figure 2. The X-ray dot map showed that the wall of the main was primarily iron consistent with a main that was made from a ferrous alloy such as steel. The fracture face contained a layer of oxygen in the form of an oxide (consistent with a layer of iron oxide).

Appendix 2C shows an X-ray dot map of a portion of soil sample “14A”. The soil sample was coated by vapor deposition with carbon. The major elements found in the soil were silicon, aluminum, calcium, oxygen, and carbon (the source of the carbon was the vapor deposited carbon coating). The EDS spectrum showed that minor elements of iron, potassium, and magnesium were found in the soil sample.

Chemical Composition of the Main

As indicated earlier, the main was installed in 1946, and cross section examination of the main revealed the main was seamless. The 1945 edition of API Standard 5L was consulted because it was the edition that was in affect at the time the steel main was installed in the ground. For the 1945 edition of the specification, the chemical composition requirements were based on whether the pipe was seamless, electric welded, or furnace butt and lap-welded. Under each of these categories, the chemical composition requirements were categorized by method of steel manufacture and further subcategorized as Grades A, B, or C. Since the NTSB Materials Laboratory examination established the pipe was seamless, discussion regarding the specified chemical composition will be restricted to materials for seamless pipe. Table 1 shows the specified amount of carbon, manganese, phosphorus, and sulfur, by percent, for seamless pipe.

One set of chemical analysis was performed by Westmoreland Mechanical & Research, Inc., Youngstown, Pennsylvania, from material at the west end portion of the main, (see Appendix 4). The chemical analysis included material that the NTSB drilled out from the main in the area adjacent to gouge "A"; refer to Materials Laboratory Factual Report 18-067 for the location of gouge "A". Another set of chemical analysis was performed by Lehigh Testing Laboratories, New Castle, Delaware, (see Appendix 4). The results of the chemical analysis are shown in table 2. Table 2 shows the results of the chemical analysis for specified and non-specified elements. The amount of nitrogen in the main was measured by weight % and hydrogen was measured in parts per million (ppm). The measured phosphorus content for the pipe and drilling samples ranged between 0.068% and 0.073%, exceeded the 0.045% max phosphorus content for most of the grades, with the exception of Bessemer Grades B and C (which permitted up to 0.11% phosphorus), see table 1. The carbon content for the main measured between 0.053% and 0.32%. Bessemer Grade B pipe material is restricted to a maximum of 0.30% carbon (measured carbon content was as high as 0.32%). However, Bessemer Grade C does not specify a carbon content. When considering only the results of the chemical composition, by process of elimination, the pipe material was consistent with Seamless Bessemer Grade C material per the 1946 edition of API Standard 5L.

Tensile Test

Three longitudinal tensile specimens were prepared from the main and tested by Westmoreland Mechanical & Research, Inc., Youngstown, Pennsylvania.[4] Table 3 shows the specified tensile values for seamless pipe and the results of the measured tensile values. The yield strength is specified for a total elongation of 0.5% of the gage length (referred as 5% extension under load [EUL]). The results of the tensile tests showed that the measured ultimate tensile strength, yield strength, and elongation values was consistent with Seamless Bessemer Grade C pipe material. The fracture face from one of the tensile specimens tested until fracture was cut to facilitate SEM examination. SEM examination of the tensile specimen fracture face revealed micro-void coalescence features typical of overstress separation.

X-ray Diffraction Analysis

Soil sample "14A" and a hard deposit that was removed from the outer surface of the main in the area indicated by bracket "B" in figure 1 of Materials Laboratory Factual Report 18-067, were analyzed by X-ray diffraction (XRD), at EAG Laboratories, Sunnyvale, California. A gouge was found on the outer surface of the main under the hard deposit "B", and the gouge under the hard deposit was arbitrarily identified as gouge "B1". The results of the X-ray analysis are shown in Appendix 3. The hard deposit referred to in the EAG report as hard deposit "B" is the same as hard deposit removed from gouge "B1", both sample designations refer to the same hard deposit sample.

[4] Each tensile specimen was manufactured with a gauge length of 2 inches and a width of 3/4 inch at the gage length, in accordance with API Standard 5L specification, 1945 edition. As indicated in the same API edition, longitudinal tensile test specimens are to be 1.5-inch wide at the gage length provided suitable curved face testing grips are employed otherwise. Lacking suitable curved face testing grips, the width of the strip specimen within the gage length shall ¾-inch wide for pipe sizes under 4-inch outside diameter.

Soil sample “14A” was analyzed to determine the crystalline phases that were present. The results of the XRD analysis was nonquantitative and reported the presence of the phases as major, minor, or trace. The results of the analysis showed that the major constituents in soil sample “14A” were calcite and quartz. The analysis also showed the presence of an x-ray pattern for montmorillonite that was similar to other phyllosilicate clays and thus the identity of this clay may not be montmorillonite. The analysis also showed a possible phase of microcline, but this phase is speculative. According the EAG Laboratories, no hydrated calcium aluminosilicate minerals were detected indicating portlandite cement was not likely present in the sample.

The hard deposit sample removed from the surface of gouge “B1” was analyzed to determine the crystalline phases that were present, and the results were reported semi-quantitative in weight percent. The results of the analysis showed that the major constituents in the hard deposit were calcite (42.9%), quartz (45.7%), clinochlore (5.6%), talc (2.5%), with possibility (speculative) phases of aragonite (1.5%), and calcium magnesium (1.7%). The tolerance on the weight percent was reported as plus or minus 5%. According to EAG Laboratories, no hydrated calcium aluminosilicate minerals were detected indicating portlandite cement is not likely present in the sample.

Size of the Main and Service Pipe

The service pipe for the dwelling at 3524 Espanola Drive was made from polyethylene. The polyethylene service pipe was connected to the steel main by a steel tee assembly. Tables 4A and 4B show the specified size and measured values of the main and service pipe. The measured diameter and thickness of main and service pipe were within the specified size.

Identification Marks Found on the Service Pipe

The outer face of the service pipe for the dwelling at 3524 Espanola Drive was marked “0218FEET F957 060397 COIL 0490 GAS USE ONLY PLEXCO® YELLOWPIPE ¾” IPS SDR11.0 PE2406 CEO ASTM D 2513 F329”. This information indicates the service pipe was manufactured on June 3, 1997 as 0.75-inch IPS pipe from medium density polyethylene, by Performance Pipe (a division of Chevron Phillips Chemical Company LP, Plano, Texas).

Location of Saw Cut Pieces

Appendix 4 show photographs of the main and the location of saw cuts that were made by the NTSB Materials Laboratory. Several saw cuts were made to remove ring sections for metallographic evaluation or to facilitate shipping portions of the main to contractor laboratories for tensile testing/chemical analysis.

Prepared by:

Frank Zakar
Senior Metallurgist

Table 1.
Chemical Composition for Seamless or Electric-Welded Pipe (Weight %)
Specified in API Standard 5L, 1945 edition

Element	Bessemer		Electric furnace			Open hearth		
	Grade B	Grade C	Grade A	Grade B	Grade C	Grade A	Grade B	Grade C
Carbon	0.30 max	Not specified	Not specified	0.30 max	Not specified	Not specified	0.30 max	Not specified
Manganese	0.35-1.5	0.35-0.5	0.30-0.90	0.35-1.50	0.35-1.50	0.30-0.90	0.35-1.50	0.35-1.50
Phosphorus	0.11 max	0.11 max	0.045 max	0.045 max	0.045 max	0.045 max	0.045 max	0.045 max
Sulfur	0.06 max	0.06 max	0.06 max	0.06 max	0.06 max	0.06 max	0.06 max	0.06 max
Iron	Remain	Remain	Remain	Remain	Remain	Remain	Remain	Remain

Table 2.
Measured Chemical Composition of Pipe
(Weight % Except Where Noted)

Element		Pipe, West End		Pipe Drilling Sample, Adjacent to Gouge "A"	
Element	Requirement, API STD 5L, 1945 edition	Westmoreland results	Lehigh results	Westmoreland results	Lehigh results
Aluminum	Not specified	-	<0.002	-	0.008
Boron	Not specified	<0.01	-	<0.01	-
Carbon	*****	**0.09**	**0.129**	**0.32**	**0.053**
Cobalt	Not specified	-	0.002	-	0.003
Chromium	Not specified	-	0.002	0.01	<0.001
Copper	Not specified	0.01	0.011	0.01	<0.001
Magnesium	Not specified	-	<0.001	-	<0.001
Manganese	**Specified**	**0.39**	**0.380**	**0.39**	**0.351**
Molybdenum	Not specified	<0.01	<0.001	<0.01	<0.001
Niobium[5]	Not specified	<0.01	-	<0.01	-
Nickel	Not specified	-	<0.001	<0.01	<0.001
Phosphorus	**Specified**	**-**	**0.068**	**-**	**0.073**
Sulfur	**Specified**	**0.041**	**0.041**	**0.041**	**0.039**
Silicon	Not specified	<0.01	0.005	0.03	0.032
Tin	Not specified	-	-	-	-
Titanium	Not specified	<0.01	-	<0.01	-
Vanadium	Not specified	0.01	0.006	0.01	0.006
Nitrogen	Not specified	0.02	0.007	0.02	0.016
Hydrogen	Not specified	3 ppm	0.0004	6 ppm	0.0006
Iron	Specified	Remainder	Remainder	Remainder	Remainder

Note: (-) indicates not reported.
(*) indicates carbon content is not specified for all the grades of steel in the 1945 edition of API STD 5L.

[5] Formerly known as the element columbium.

Table 3. Tensile Properties of the Base Metal for Seamless Pipe per API Standard 5L,1945 Edition						
Property	Specified Minimum			Measured		
	Grade A (for measured thickness 0.156 inch)	Grade B (for measured thickness 0.156 inch)	Grade C	Specimen #1	Specimen #2	Specimen #3
Yield Strength, 0.5% EUL, (psi)[6]	30,000	35,000	45,000	63,500	65,000	65,000
Ultimate Tensile Strength (psi)	48,000	60,000	75,000	85,100	84,900	84,900
Elongation (%)	26.25	22.5	20	28	28	28

Table 4A Outer Diameter (Inches)				
Pipe	Specified	Method of Measure	Measured	
			3539 Durango Dr	3524 Espanola Dr
PE 3/4-inch IPS Nominal Tubing Size	1.046-1.054 (per ASTM D2513-87)	Caliper	Not Applicable	1.052
Steel 2-3/8 inch OD Nominal Pipe	2.35-2.39 (per Standard 5L, 1945 Edition)	Caliper	2.4	2.4

Table 4B Thickness (Inches)				
Pipe	Specified	Method of Measure	Measured	
			3539 Durango Dr	3524 Espanola Dr
PE 3/4-inch IPS Nominal Tubing Size	0.095-0.106 (per ASTM D2513-87)	Caliper	Not Measured	0.1
Steel 2-3/8 inch OD Nominal Pipe	0.13 - 0.18 (per Standard 5L) 1945 Edition	Ball-Flat Micrometer	0.167	0.15

[6] Extension under load (EUL) method - stress required to produce a total elongation of 0.5% of the gage length.

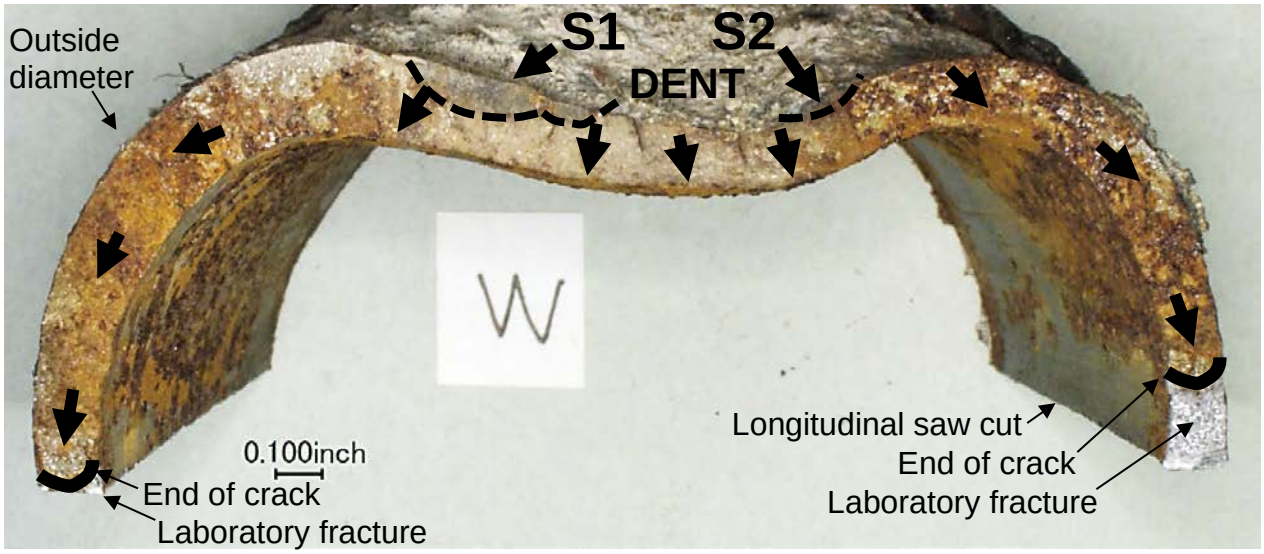

Figure 1. West face of the fracture after separating the mating faces of the circumferential crack, prior to cleaning. General direction of fracture propagation is indicated by unmarked arrows and termini of crack is indicated by a solid lines.

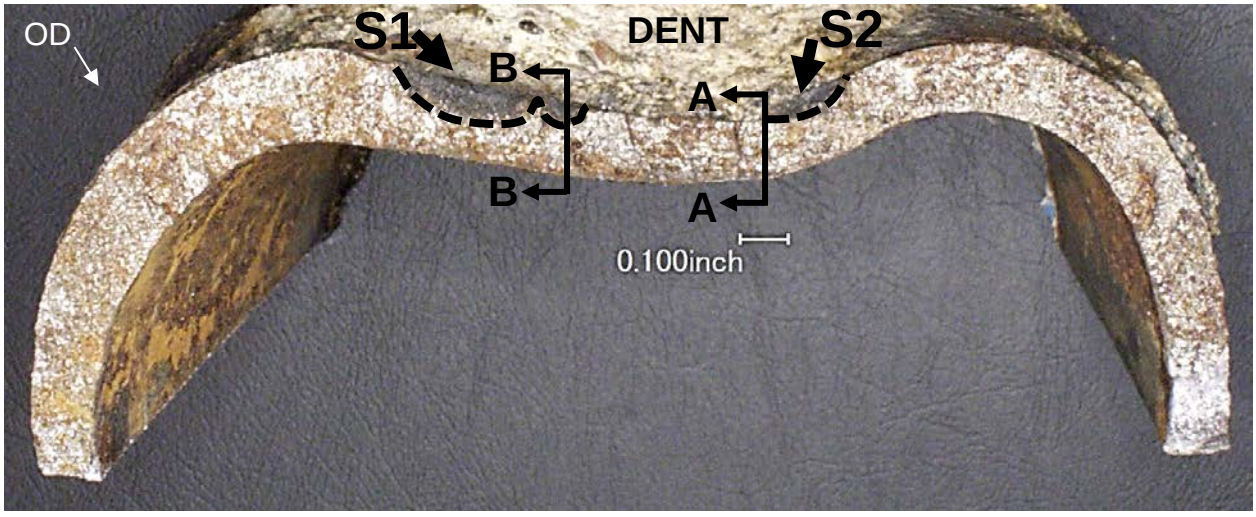

Figure 2. West face of the fracture, after the replica tape cleaning procedure was repeated four times, exposing black regions “S1” and “S2”. Refer to the previous figure to determine the relative positions of the black regions prior to fracture cleaning.

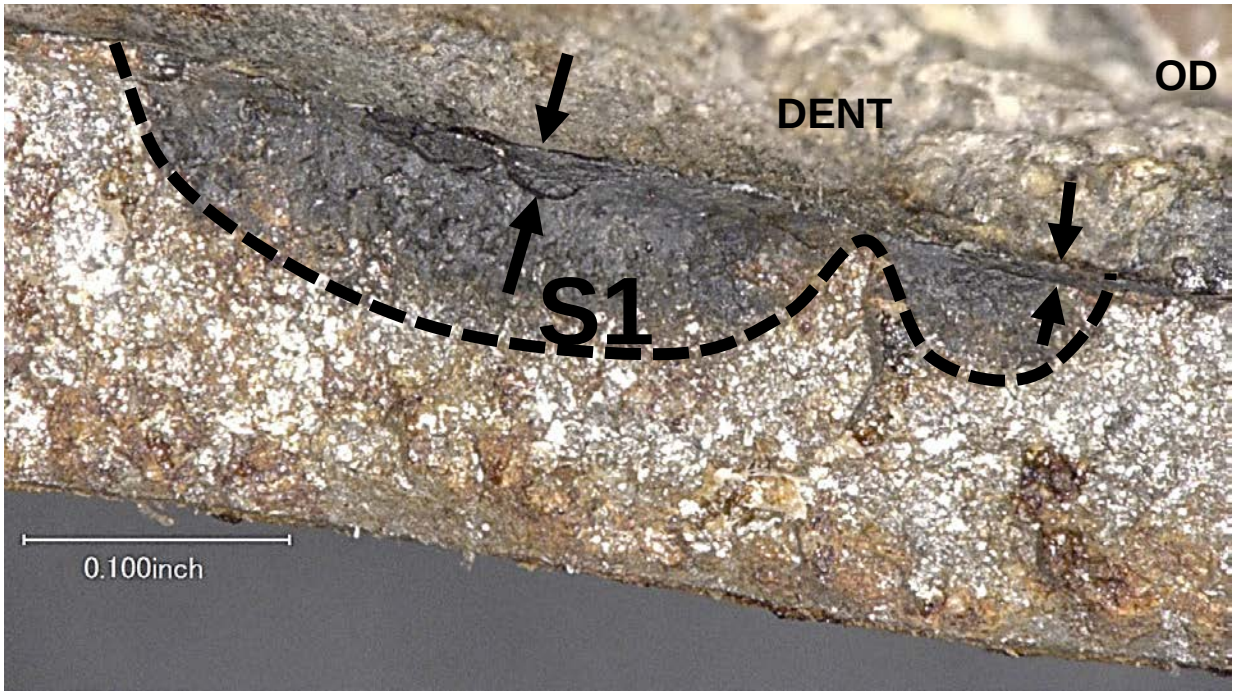

Figure 3. Close-up view of black region “S1” in figure 2. Minor shear lips on outer face of fracture are located between arrows.

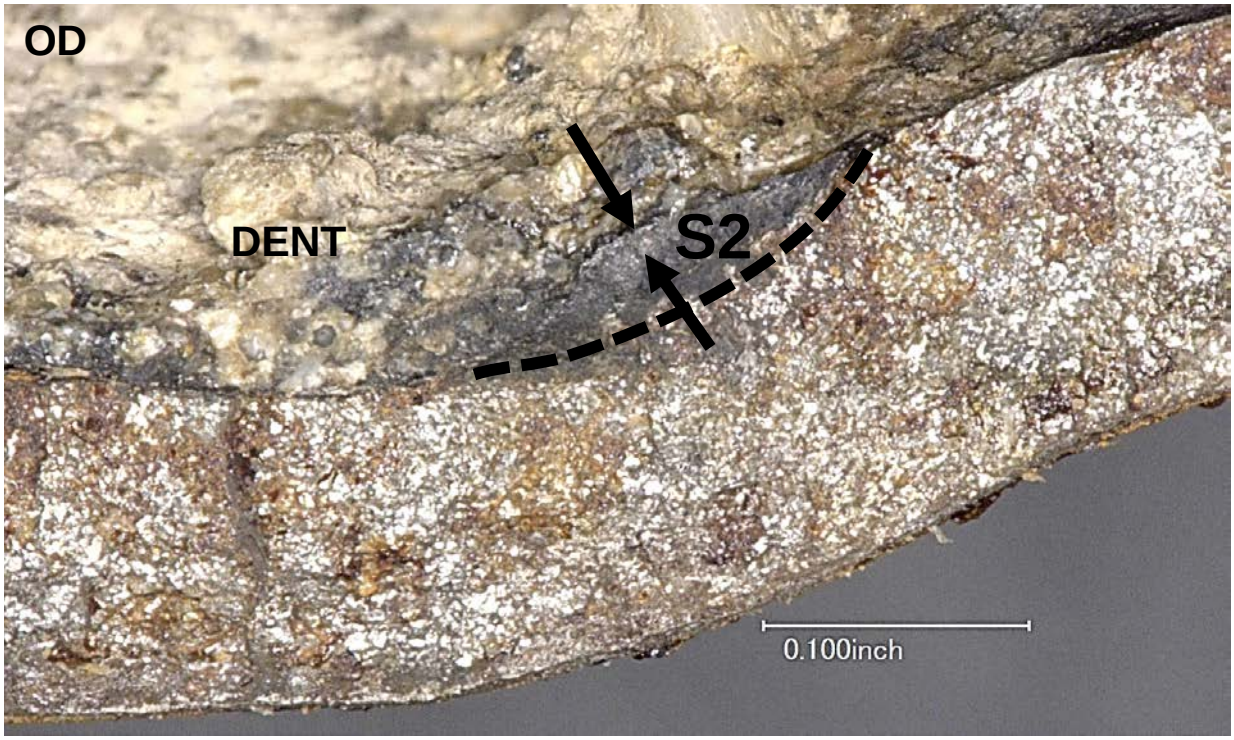

Figure 4. Close-up view of black region “S2” in figure 2. Minor shear lips on outer face of fracture are located between arrows.

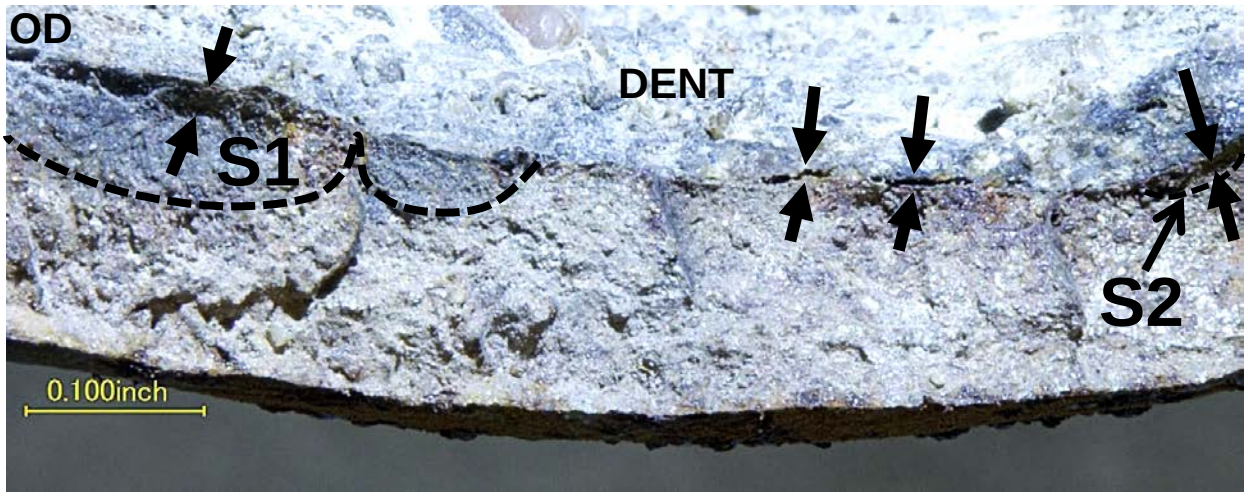

Figure 5. West face of the fracture in the area near the center of the dent. In this image, side lighting highlighted minor shear lips at the outer surface between unmarked arrows.

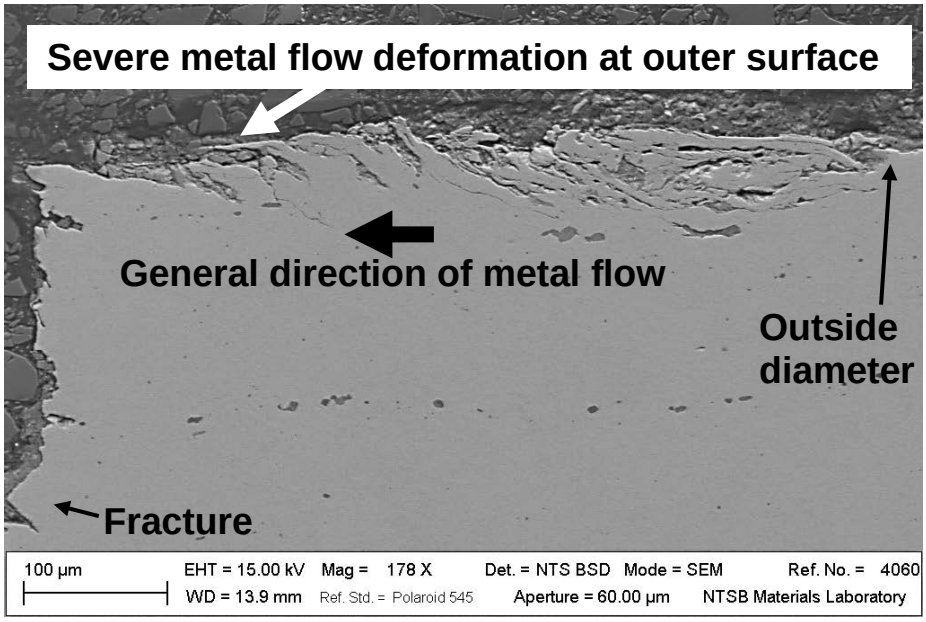

Figure 6. SEM image of a cross section "A-A" in figure 2 in an area adjacent to the fracture showing severe metal flow deformation at the outer surface, as-polished. Metal flow deformation is toward the fracture in the direction indicated by an arrow.

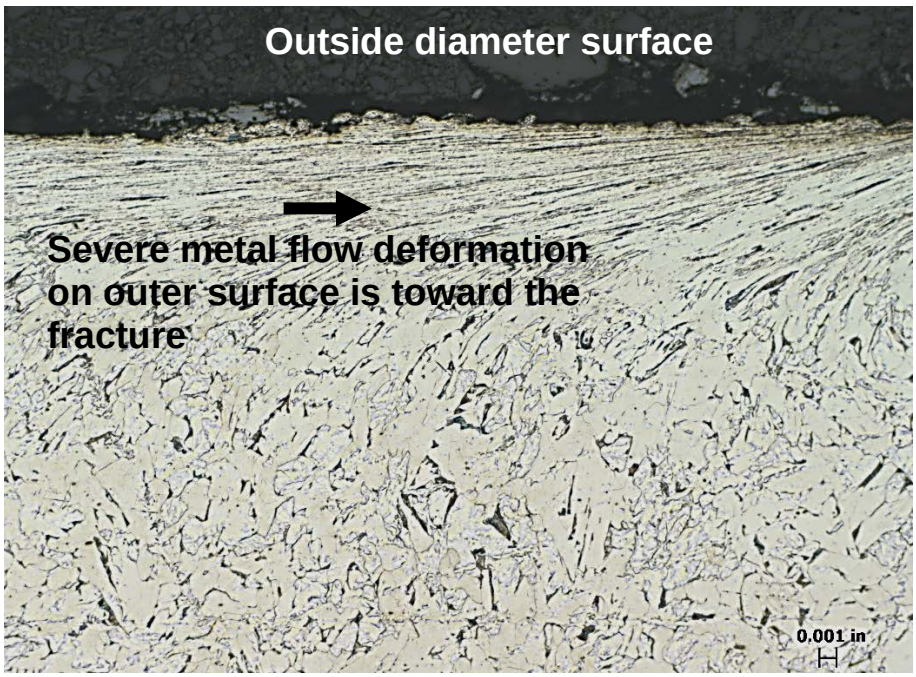

Figure 7. Cross section "A-A" showing metal flow deformation at the outer diameter surface in an area near the fracture but outside of the region shown in figure 6. Metal flow deformation is toward the fracture in the direction indicated by an arrow. The metallographic cross section shown above was made on a Zeiss metallograph that produces a mirror image of actual cross section, thus, metal flow deformation shown here is in opposite direction of SEM image. Etched with 2% Nital.

APPENDIX 1

EDS Spectra

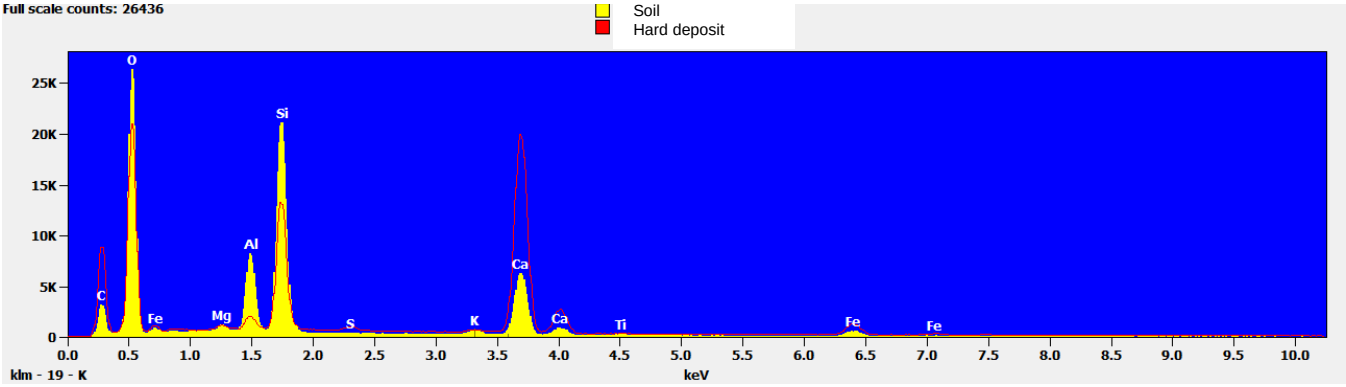

Appendix 1A. EDS spectrum of soil sample “14A” (solid yellow) overlapped with EDS spectrum of hard deposit found on top of gouge “B1” (red outline).

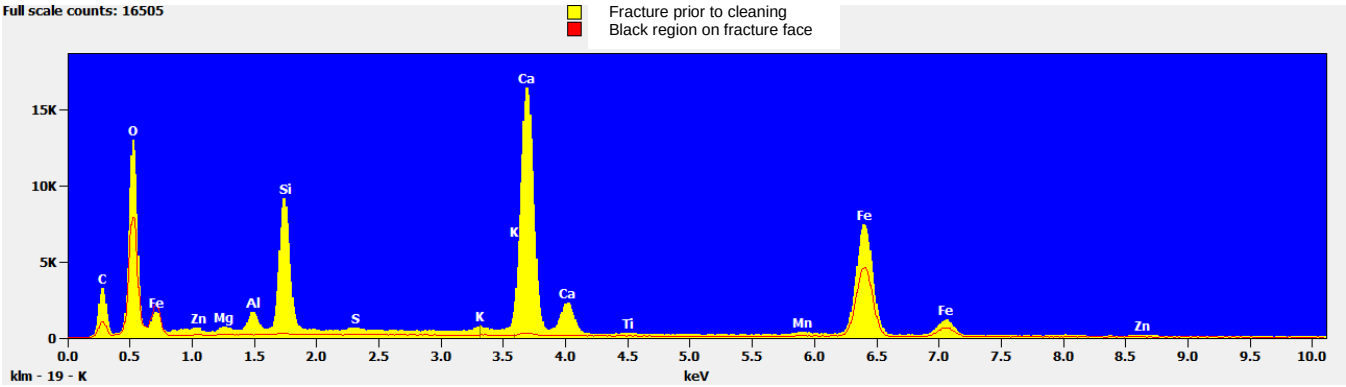

Appendix 1B. EDS spectrum of fracture face prior to cleaning (solid yellow) overlapped with EDS spectrum of fracture face after cleaning with replica tape and exposing black region “S1” (red outline).

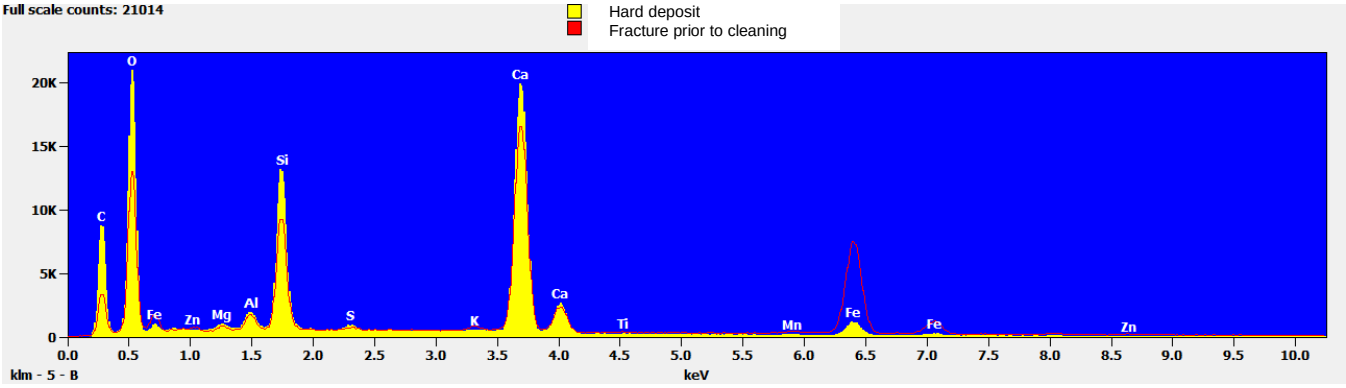

Appendix 1C. EDS spectrum of hard deposit found on top of gouge “B1” (solid yellow) overlapped with EDS spectrum of fracture face prior to cleaning (red outline).

APPENDIX 2

X-ray Dot Maps of Hard Deposit, Fracture Face, and Soil Sample “14A”

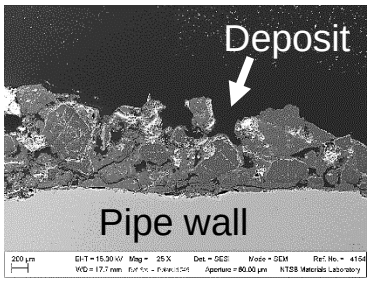

SEM image

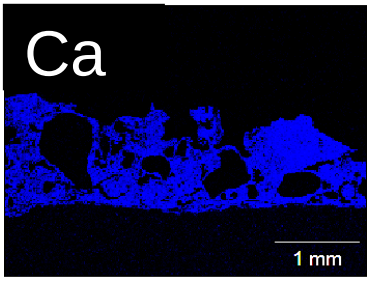

X-ray dot map for Ca

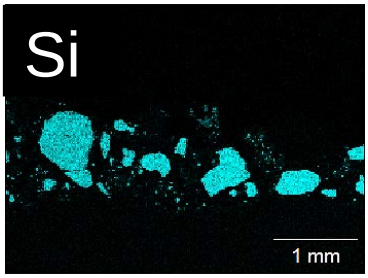

X-ray dot map for Si

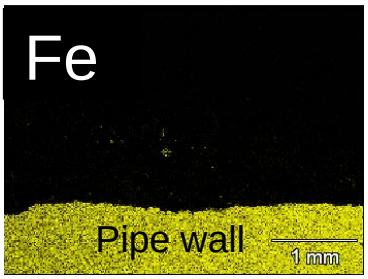

X-ray dot map for Fe

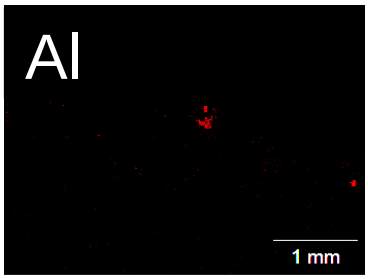

X-ray dot map for Al

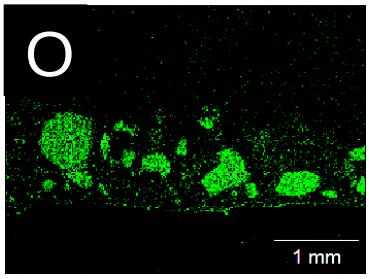

X-ray dot map for O

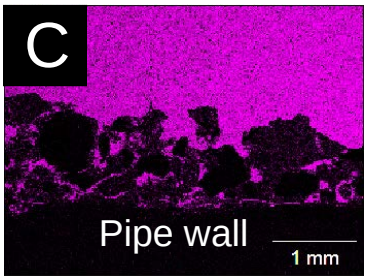

X-ray dot map for C

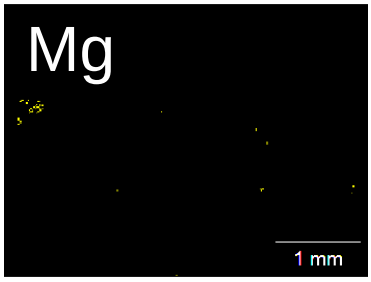

X-ray dot map for Mg

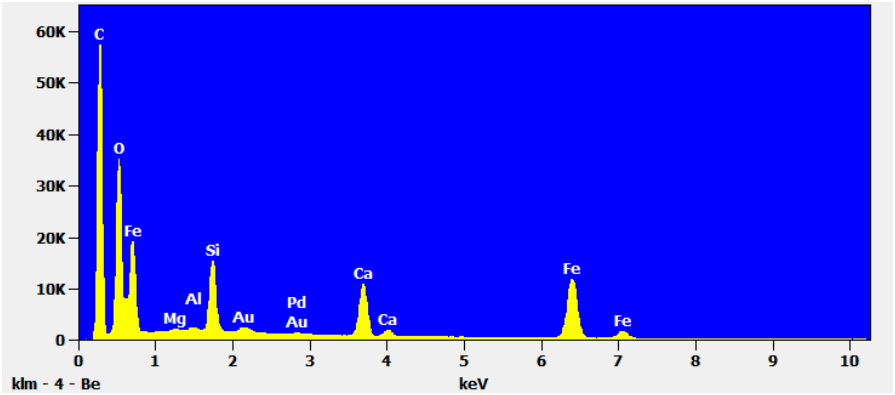

Appendix 2A. X-ray dot map (upper images) and spectrum (lower image) of the hard deposit that was found on the outer surface of the main in the area indicated by section line “B-B” in figure 2. Section was mounted in transparent plastic and coated by vapor deposition method with gold-palladium to prevent charging in the SEM.

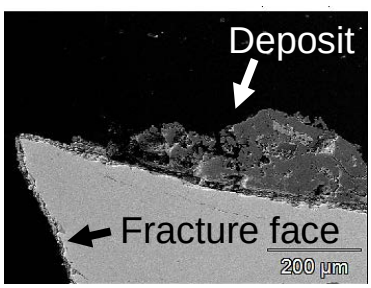

SEM image

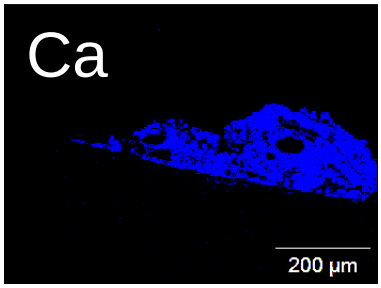

X-ray dot map for Ca

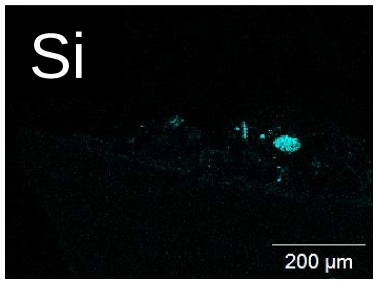

X-ray dot map for Si

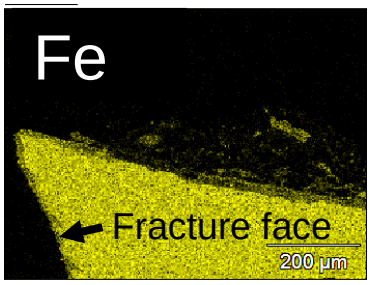

X-ray dot map for Fe

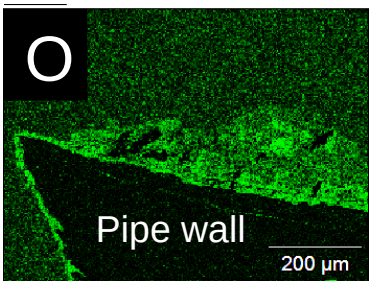

X-ray dot map for O

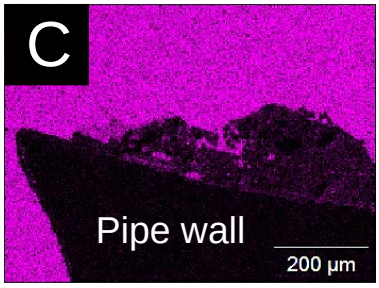

X-ray dot map for C

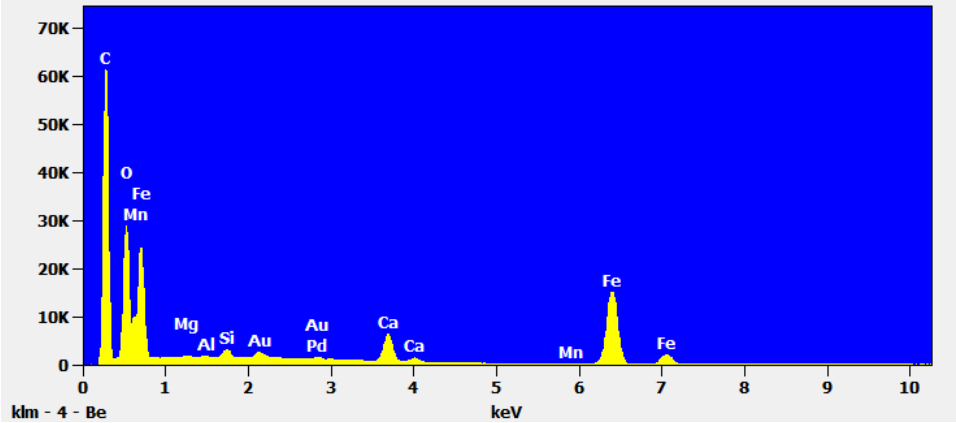

Appendix 2B. X-ray dot map (upper images) and spectrum (lower image) of the fracture face where it intersected the outer surface of the main in the area indicated by section line “B-B” in figure 2. Section was mounted in transparent plastic and coated by vapor deposition method with gold-palladium to prevent charging in the SEM.

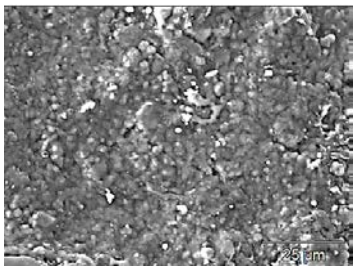

SEM image

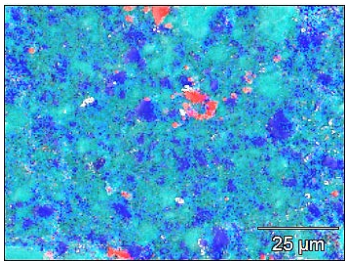

X-ray dot map showing overlap for elements Si, Ca, and Al

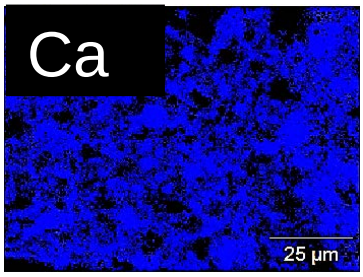

X-ray dot map for Ca

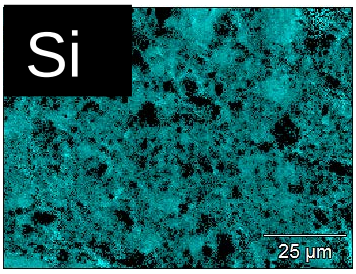

X-ray dot map for Si

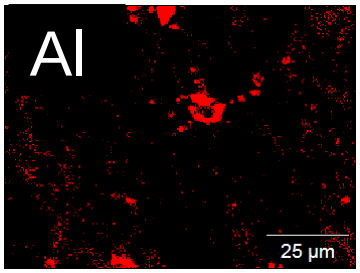

X-ray dot map for Al

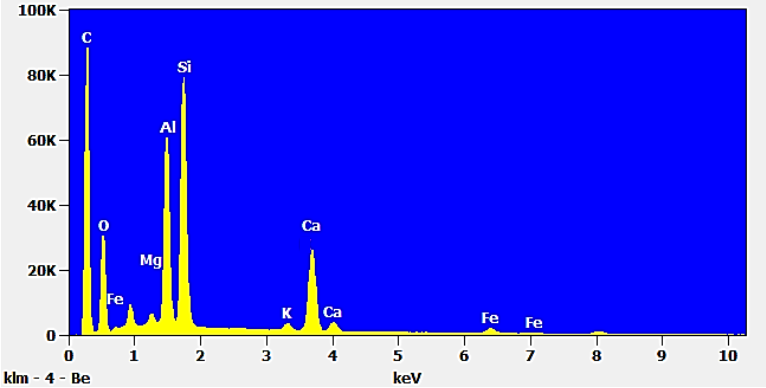

Appendix 2C. X-ray dot map (upper images) and spectrum of soil sample “14A” showing the distribution of individual major elements. The sample was coated by vapor deposition method with carbon to prevent charging in the SEM.

APPENDIX 3

EAG Laboratories
X-Ray Diffraction (XRD) Analysis Report
Dated 06 Dec 2018
(8 Pages)

ISO 17025

Testing Cert. #2797.01

X-RAY DIFFRACTION (XRD) ANALYSIS REPORT
06 Dec 2018

JOB NUMBER C0JAD726
PO NUMBER Credit Card

for

Frank Zakar
National Transportation Safety Board

Prepared by:

[redacted]

_____
William R. Woerner, Ph.D.
Senior Scientist
[redacted]

Reviewed by:

[redacted]

_____
Wes Nieveen
Scientific Fellow
[redacted]

EAG Laboratories
810 Kifer Rd
Sunnyvale, CA 94086-5203 USA

Requester: Frank Zakar
Job Number: C0JAD726
Analysis Date: 06 Dec 2018

X-RAY DIFFRACTION ANALYSIS REPORT

Purpose: Use X-ray diffraction to identify the phases present in a soil sample and quantify the phases present in the possible cement sample. The samples are identified in the table below.

Summary:

Table 1: Phase Identification from the ICDD/ICSD databases

Sample ID	Primary Phases	Concentration (± 5 wt%)
Soil 14A	$CaCO_3$ – Calcite Hexagonal, SG: R-3c (167) PDF# [04-012-0489] SiO_2 – Quartz Hexagonal, SG: P3221 (154) PDF# [98-000-0369] $Ca_{0.2}(Al,Mg)_2Si_4O_{10}(OH)_2 \bullet 4H_2O$ – Montmorillonite – 15A ** Hexagonal PDF# [00-013-0135] $KAlSi_3O_6$ – Microcline **??** Triclinic, SG: C-1 (2) PDF# [98-000-0305]	-
Hard Deposit B	$CaCO_3$ – Calcite Hexagonal, SG: R-3c (167) PDF# [04-012-0489] SiO_2 – Quartz Hexagonal, SG: P3221 (154) PDF# [98-000-0369] $Mg_5Al_2Si_3O_{18}H_8$ – Clinochlore Monoclinic, SG: C2/m (12) PDF# [98-000-3761] $Mg_3Si_4O_{12}H_2$ – Talc Triclinic, SG: C-1(2) PDF# [98-001-3304]	42.9 45.7 5.6 2.5

	$CaCO_3$ – Aragonite **??** Orthorhombic, SG: Pmcn (62) PDF# [98-000-7788]	1.5
	$CaMg(CO_3)_2$– Calcium magnesium carbonate (dolomite) **??** Hexagonal, SG: R-3 (148) PDF# [04-015-9853]	1.7

**** - The XRD pattern for montmorillonite is very similar to other phyllosilicate clays and thus the identity of this clay may not be montmorillonite.**

?? – Speculative phase identification

Results and Interpretations: The as-received samples were ground in a mortar and pestle to homogenize the samples. The resulting powders were packed into a bulk sample holder and pressed flat with a glass slide for analysis. XRD data was collected by a coupled theta: two-theta scan on a Rigaku SmartLab diffractometer equipped with copper X-ray tube with Ni beta filter, parafocusing optics, computer-controlled slits, and D/TeX HE 1D strip detector.

The phase identification results are summarized in Table 1. Figures 1 and 2 compare the best matches between the background-modelled experimental XRD data to the ICDD/ICSD diffraction database for the samples. The reference markers for the phase show where in two-theta the expected experimental peaks should be located and the height of the markers indicates the expected intensity of the experimental peaks, if the sample is fine-grained and randomly oriented. Note that XRD is sensitive to crystal structure but relatively insensitive to elemental or chemical state composition. No hydrated calcium aluminosilicate minerals were detected in either sample indicating portlandite cement is likely not present in the samples.

Semi-quantitative analysis for sample Hard Deposit B was performed using WPF (Whole Pattern Fitting), which is a subset of Rietveld Refinement that accounts for all intensity above the background curve. This technique requires that either the structure factors and atomic locations or the reference intensity ratio (a way of comparing the diffracting power of different phases) are known for all phases identified. During this process, structure factor (which relates to concentration), lattice parameters (which relate to peak position), peak width and peak shape are refined for each phase to minimize the R value – an estimate of the agreement between the model and the experimental data over the entire pattern.

The whole pattern fitting results are shown in Figure 3 with a summary of the results included in Table 1. The R value of 5.56% indicates a good fit between the experimental data and refined pattern.

After reviewing this report, you may assess our services using an electronic service evaluation form. This can be done by clicking on the link below, or by pasting it into your internet browser. Your comments and suggestions allow us to determine how to better serve you in the future.
http://www.eag.com/main-survey.html?job=C0JAD726

If you would like to run further analyses on samples like those for which you have just received data, please click here: http://www.eag.com/customer-portal.html to generate a new job number and reserve your place in our queue. A customer service representative will contact you to confirm details with you soon after you fill out the short form.

For your other analytical needs please click here: http://www.eag.com/mc/contact-us-mc.html

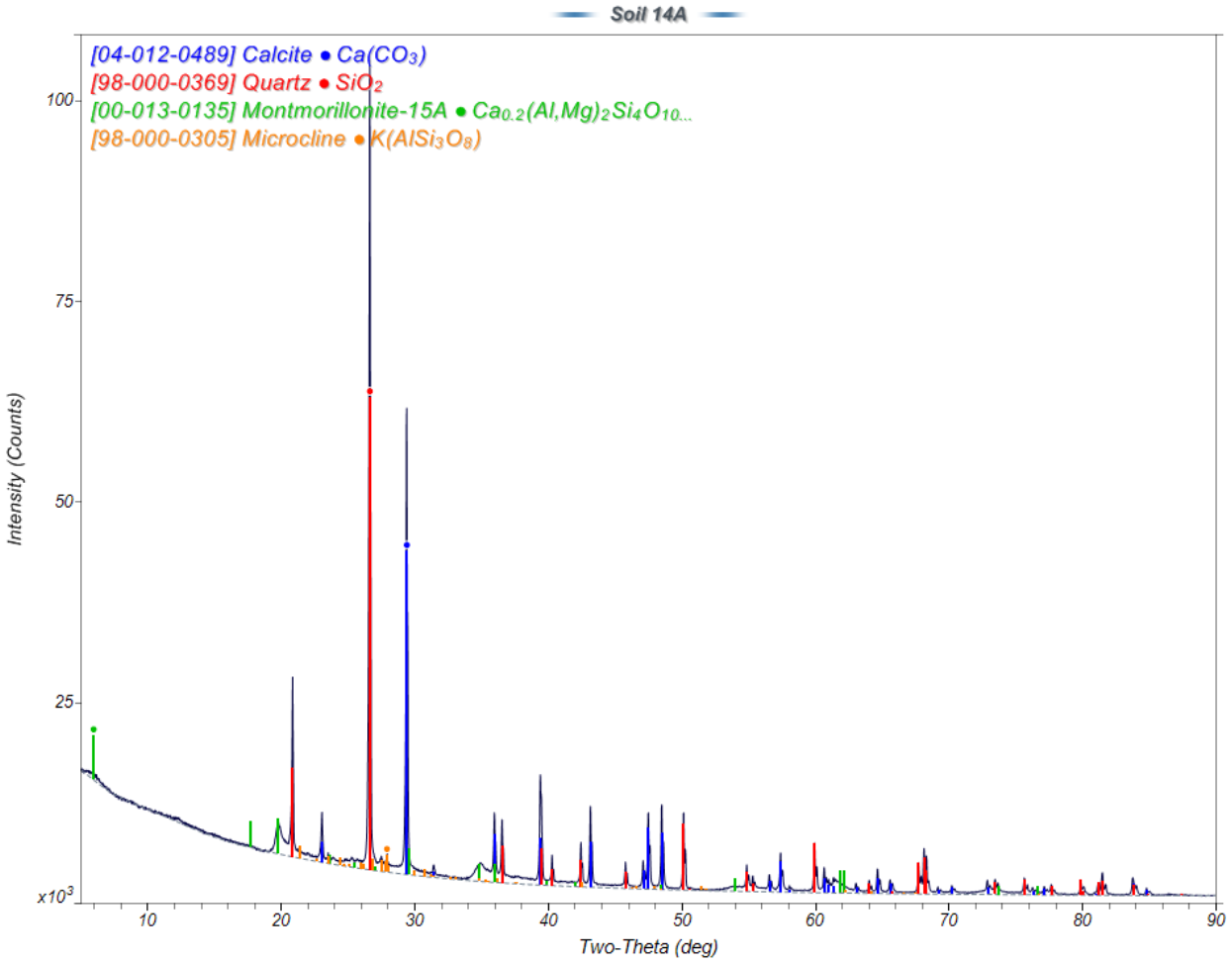

Figure 1: Phase identification results for sample Soil 14A

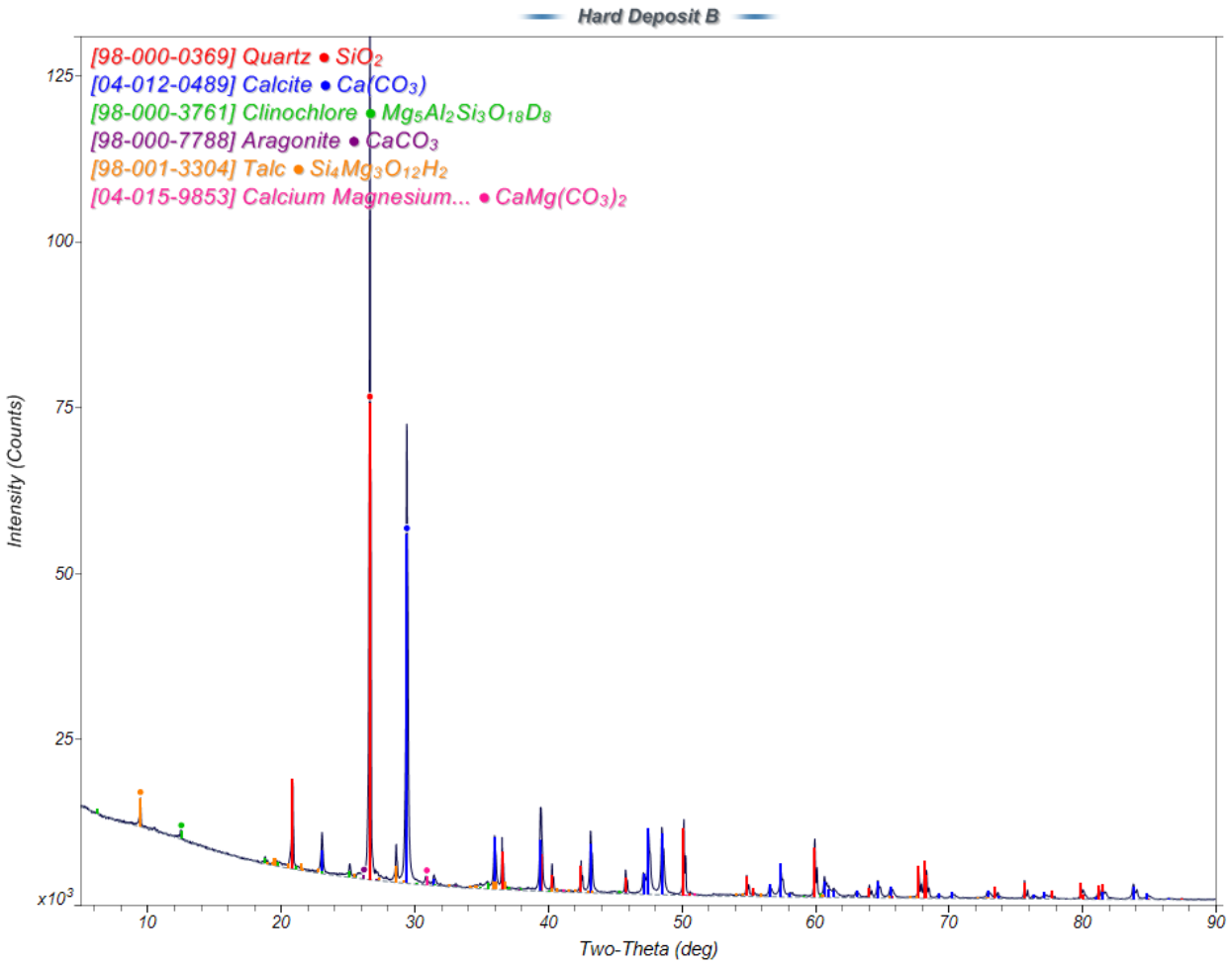

Figure 2: Phase identification results for sample Hard Deposit B

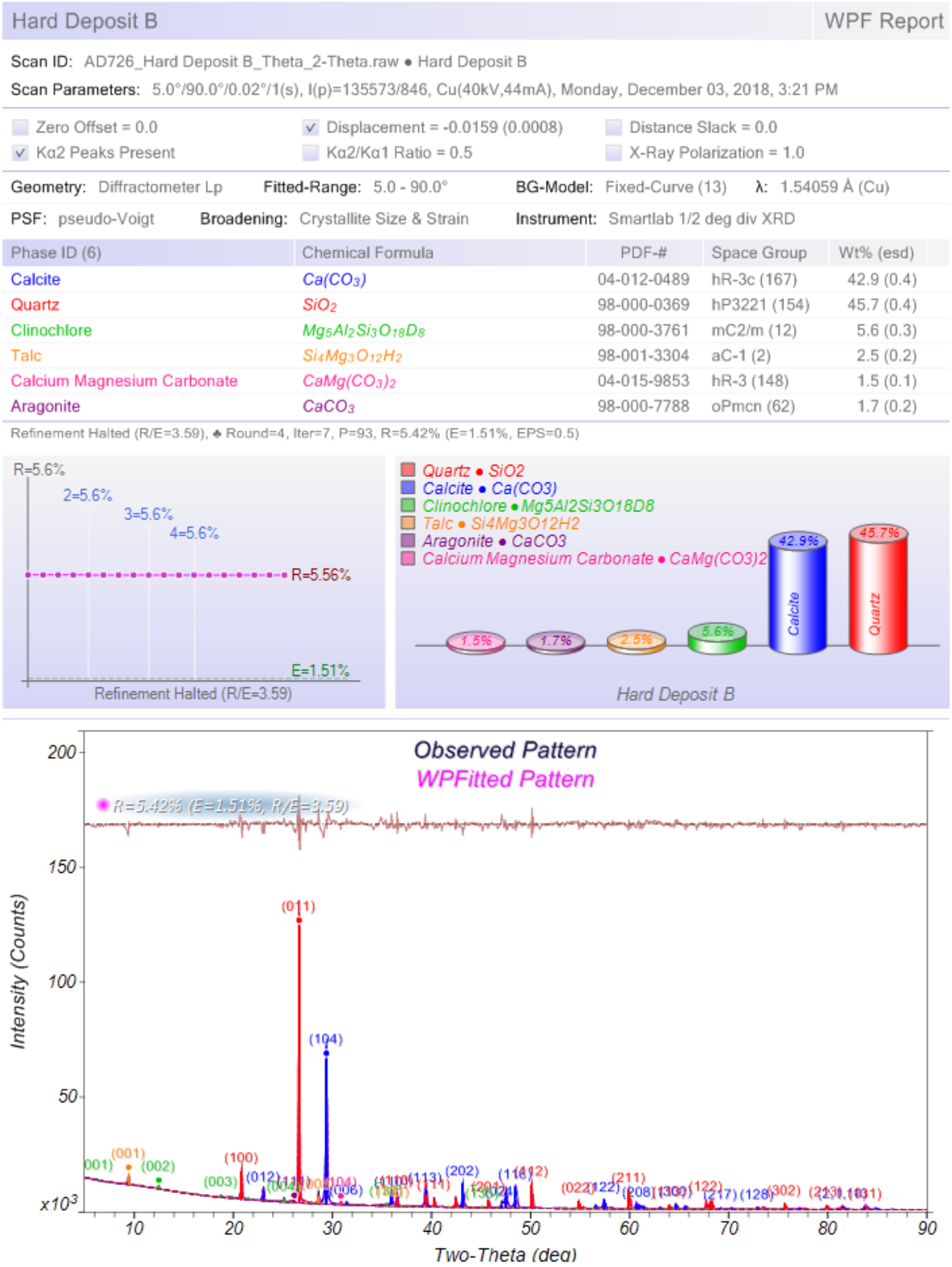

Figure 3: Whole pattern fitting results for sample Hard Deposit B

Appendix

Measurement Uncertainty:

There are two types of uncertainty in XRD analysis; uncertainty in the number of X-ray counts at a particular angle and uncertainty in the diffraction angle. Because the arrival of X-ray quanta in the detector is random with respect to time, the accuracy of X-ray counting rate measurements is governed by the laws of probability. In particular, the size of the one sigma standard deviation in an X-ray measurement is equal to the square root of the number of X-rays counted. A conservative criterion for the detection of a weak peak in a XRD pattern must have amplitude of greater than three standard deviations above background. As a result, the more slowly a measurement is made, the lower the relative standard deviation in the number of counts measured and the more likely is detection of trace diffraction peaks. If X-ray data is acquired at a constant speed, the relative standard deviation for the major diffraction peaks in a pattern will be on the order of a few percent or less while the relative standard deviation for the weaker peaks in a pattern will be on the order of tens of percent or more. This also implies that the uncertainty in the concentrations of the major phases in a sample will be lower than for the trace phases. Please note that there are a number of sample related factors that can influence peak intensity. These include (but are not limited to): average crystallite size, preferred orientation (texture), strain, and absorption.

Uncertainty in the position of X-ray diffraction peaks is due to both instrumental and sample effects. Instrumental position uncertainty is primarily due to diffractometer misalignment. Repeat measurements of NIST standard reference materials has shown that the maximum positional uncertainty is less than +/- 0.05 degrees 2-Theta and is typically much less than that. Positional uncertainty due to sample effects are related to sample displacement (displacement of the sample surface either above or below the diffractometer focusing circle) and sample transparency (the effect gets larger as the sample matrix becomes more transparent to the incident X-rays. Through careful sample preparation, the uncertainty due to these two sample effects should be less than +/- 0.03 degrees 2-Theta. Please note that in addition to these factors, solid solution effects, where one element is partially substituted for another within a given crystal structure, can produce significant shifts in measured peak positions. Unlike sample and instrumental peak position effects, solid solution effects can result in phase misidentification.

APPENDIX 4

Main
Saw Cut Locations
(1 Page)

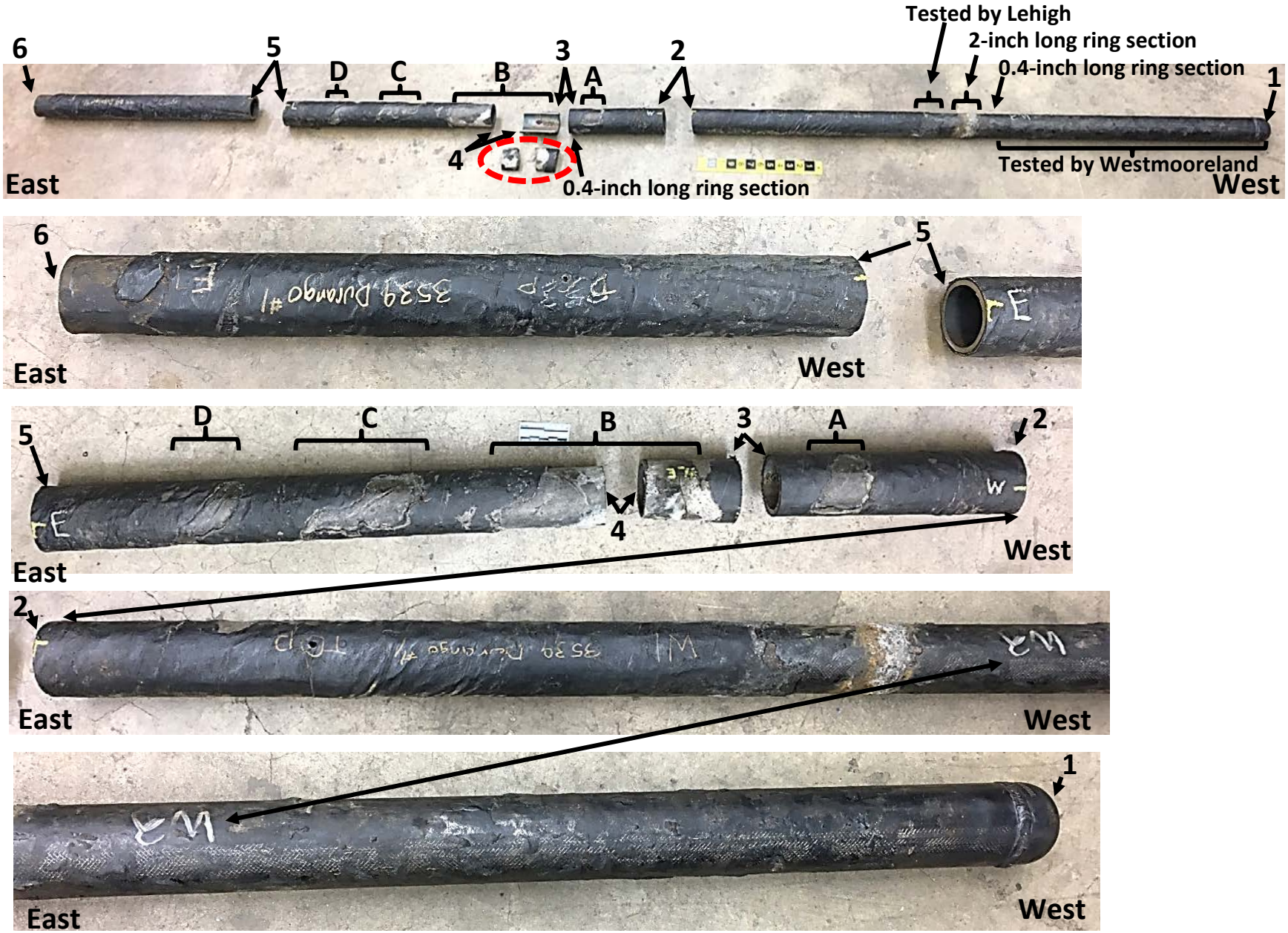

Appendix 4. Photographs of the 10-foot main segment of the main that was located behind dwelling 3539 Durango Drive showing exposed areas with damaged coating indicated by brackets "A", "B", "C", and "D". Saw cuts made by NTSB lab are identified by arrows "2" through "5". Field cut is identified by arrow "6". Weld cap end made on-site is indicated by arrow "1". Ring sections cut by NTSB lab and portions tested by Lehigh and Westmoreland laboratories are indicted on the top photograph. Area "B" contains the dent and crack. Dashed circle indicates location where a longitudinal saw cut was made by NTSB lab through the main causing the top half of the main to separate from the bottom half and exposing the crack that intersected dent "B". Refer to NTSB Materials Laboratory Factual Report No. 18-067 for photographs of the as-received main segment.